

# DECOMPOSING TRENDS IN U.S. AIR POLLUTION DISPARITIES FROM ELECTRICITY

Danae Hernandez-Cortes, Kyle C. Meng, and Paige Weber\*

May 2022

## Abstract

This paper quantifies and decomposes recent trends in U.S. PM<sub>2.5</sub> disparities from the electricity sector using a high-resolution pollution transport model. Between 2000-2018, PM<sub>2.5</sub> concentrations from electricity fell by 87% for the average individual, more than double the decline rate in overall U.S. ambient PM<sub>2.5</sub> concentrations. Across racial/ethnic groups, we detect a dramatic convergence: since 2000, the Black-White PM<sub>2.5</sub> disparity from electricity has narrowed by 94% and the Hispanic-White PM<sub>2.5</sub> disparity has narrowed by 92%, though these disparities still exist in 2018. A decomposition exercise reveals nearly all of these disparity trends can be attributed to spatially-varying improvements in emissions intensities, with small contributions from scale, compositional, and residential location changes. This suggests local air pollution policies have played a larger role in reducing U.S. racial/ethnic pollution disparities from electricity than recent coal-to-natural gas fuel switching. While we detect similarly large PM<sub>2.5</sub> improvements for the average low and high income individual, PM<sub>2.5</sub> differences by income are relatively small and have changed little over time.

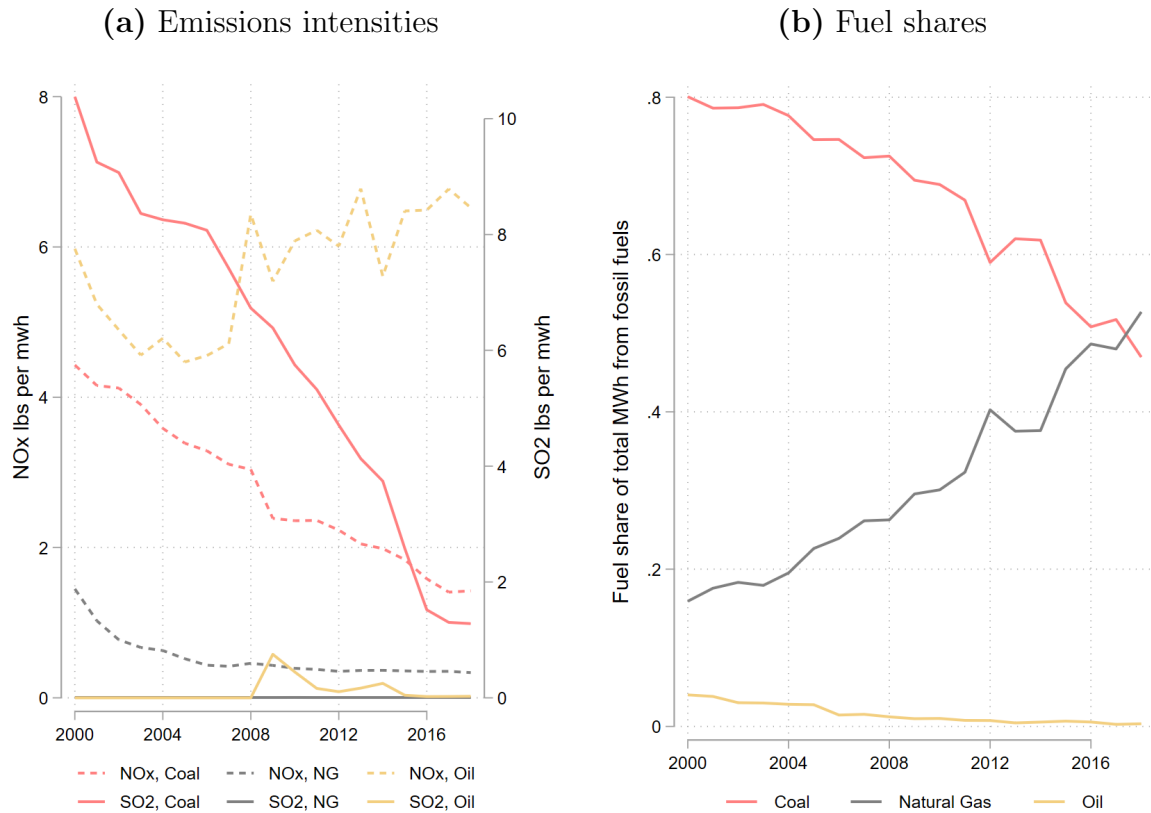
---

\*Hernandez-Cortes: Arizona State University, Danae.Hernandez-Cortes@asu.edu, Meng: University of California, Santa Barbara and NBER, kmeng@ucsb.edu, Weber: University of North Carolina at Chapel Hill, paigeweber@unc.edu. We thank Risa Lewis and Alexander Abajian for outstanding research assistance. We thank Christopher Tessum for valuable comments.

# 1 Introduction

Over the last two decades, the U.S. electricity sector has undergone two dramatic transformations. Between 2000-2018, the emissions intensity for air pollution, defined as emissions per output, has decreased, most notably for coal-fired electricity. As Figure 1a shows, emissions intensity from coal in 2018 fell to one-half of its 2000 value for nitrogen oxides ( $\text{NO}_x$ ) and one-quarter of its 2000 value for sulfur dioxide ( $\text{SO}_2$ ).<sup>1</sup> During this same period, the share of fossil-fuel electricity produced from coal has fallen while the share from natural gas has risen, with shares of the two fuels crossing in 2017, as shown in Figure 1b.

**Figure 1:** U.S. electricity air pollution emissions intensities and fuel shares over time



**Notes:** Panel (a) shows 2000-2018 annual emissions intensity (in lbs per mwh) averaged across fossil fuel-fired electricity generating units by coal, natural gas, and oil for  $\text{NO}_x$  (dashed lines) and  $\text{SO}_2$  (solid lines). Panel (b) shows share of U.S. electricity generation from fossil fuels by coal, natural gas, and oil.

These two developments have potentially important consequences for local air pollution concentrations and its distribution across the country. The U.S. electricity sector is a major

<sup>1</sup>Similar declining emissions intensity trends have been detected from U.S. manufacturing (Levinson, 2009; Shapiro and Walker, 2018).

source of criteria air pollution:<sup>2</sup> in 2000, electricity contributed 16% of overall U.S. ambient PM<sub>2.5</sub> concentrations. Its pollution is also unevenly distributed across demographic groups (EPA, 2018; Thind et al., 2019), a pattern that is broadly consistent with an extensive environmental justice literature documenting higher air pollution concentrations in locations where individuals from minority groups, and/or with low income reside.<sup>3</sup>

A question of growing concern is whether such pollution disparities from U.S. electricity have changed over time and if so, along which demographic dimensions and why. Pollution disparities depend on where power plants are located, where households from each demographic group reside, and the pollution transport patterns that disperse pollution from plants onto households. Trends in pollution disparities therefore depend on how the spatial distributions of each of these component evolve over time. In particular, the aggregate emissions intensity improvements and fuel switching shown in Figure 1 are unlikely to be evenly distributed across the country. For example, nonattainment counties regulated under the US Clean Air Act, which has been attributed with emissions intensity improvements in manufacturing (Shapiro and Walker, 2018), tend to be spatially concentrated in certain parts of the country. Likewise, local variation in coal and natural gas prices should induce more coal-to-natural gas switching in some places than others.

An understanding of these drivers can inform future policies. For example, reduced air pollution disparities due to improvements in emissions intensities would suggest a reliance on local air pollution policies, such as the U.S. Clean Air Act, for reducing future air pollution disparities. On the other hand, if recent coal-to-natural gas fuel switching did more to improved air pollution disparities, future climate policies that similarly make carbon-intensive fuels more expensive may jointly reduce GHG emissions and local air pollution disparities, as GHGs and local pollutants are often co-emitted. Indeed, both types policies have been shown to reduce air pollution disparities in other settings. Currie, Voorheis and Walker (2021) demonstrate that 60% of the recent convergence in ambient air pollution disparity between Black and White households can be attributed to the U.S. Clean Air Act. In California, Hernandez-Cortes and Meng (2022) find that the state's GHG cap-and-trade program reduced local air pollution disparities from industrial sources.

This paper quantifies U.S. PM<sub>2.5</sub> concentration trends from electricity during 2000-2018 by demographic group. Specifically, we convert annual air pollution emissions from the near-universe of U.S. fossil fuel electricity generating units into resulting PM<sub>2.5</sub> concentrations for

---

<sup>2</sup>The US EPA considers the following as criteria pollutants: ground-level ozone, particulate matter, carbon monoxide, lead, sulfur dioxide, and nitrogen dioxide.

<sup>3</sup>Disparities across various air pollutants in the U.S. have been documented through case studies (Bullard, 2000; Bowen, 2002; Ringquist, 2005; Mohai, Pellow and Roberts, 2009; Banzhaf, Ma and Timmins, 2019) and population-level studies (Colmer et al., 2020; Currie, Voorheis and Walker, 2021).

the average individual in each demographic group using a high spatial resolution pollution transport model.<sup>4</sup> We then decompose pollution disparity trends into changes in the overall scale of fossil fuel electricity generation, emissions intensities, the composition of generating units - which incorporates fuel switching within generators and the entry and exit of generators - and where individuals of different demographic groups reside.

Our analysis reveals several new facts. First, PM<sub>2.5</sub> concentrations from U.S. electricity generation fell by 87% for the average U.S. individual during 2000-2018, more than double the rate of decline in overall U.S. ambient PM<sub>2.5</sub> concentrations (from all pollution sources) during the same period. To put this in context, in 2000 PM<sub>2.5</sub> concentrations from electricity was 16% of U.S. ambient PM<sub>2.5</sub> concentrations; in 2018, that percentage was 3.5%. This large pollution decline was shared across racial/ethnic groups: PM<sub>2.5</sub> concentrations from electricity fell by 89%, 84%, and 87%, for the average Black, Hispanic, White individual, respectively. Second, the dispersion in PM<sub>2.5</sub> concentrations across racial/ethnic groups has converged dramatically. While the average Black individual consistently experienced higher PM<sub>2.5</sub> concentrations than the average White individual, this PM<sub>2.5</sub> gap fell from 0.71 to 0.04  $\mu/m^3$ /person during 2000-2018, a drop of 94%. The average Hispanic individual consistently experienced lower PM<sub>2.5</sub> concentrations than the average White individual, and this gap has narrowed by 92% from -0.96 to -0.08  $\mu/m^3$ /person during this period. These disparities, however, still exist in 2018. Third, in a decomposition exercise, nearly all of the trends in Black-White and Hispanic-White PM<sub>2.5</sub> disparities can be attributed to changes in local pollution emissions intensities. Neither scale changes, compositional changes across generators, nor changes in where people live account for much of the overall trends in PM<sub>2.5</sub> disparities. Fourth, PM<sub>2.5</sub> concentrations for the average bottom and top decile individual fell by 87% and 89%, respectively, during this period. However, in contrast to racial/ethnic disparities, PM<sub>2.5</sub> differences by income are relatively small and have changed little since 2000.

Our analysis combines two methodological approaches. Any attribution of the origins of pollution concentrations must account for how pollution from emitting facilities (sources) alters concentrations in exposed locations (receptors). The conventional approach is for researchers to assume simple spatial patterns, such as allowing pollution to only affect areas within a facility's geographic unit or within a surrounding distance-based circle. Actual pollution dispersal patterns, however, are far more spatially complex, which, when overlooked may lead to biased pollution disparity results (Deschenes and Meng, 2018; Hernandez-Cortes

---

<sup>4</sup>Power plants emit local pollutants such as NO<sub>x</sub>, SO<sub>2</sub>, and particulate matter directly. Our data only covers NO<sub>x</sub> and SO<sub>2</sub> emissions. Our pollution transport model uses atmospheric chemical relationships to convert these primary NO<sub>x</sub> and SO<sub>2</sub> emissions into resulting secondary particulate matter of 2.5 micrometers and smaller (PM<sub>2.5</sub>). The majority of ambient PM<sub>2.5</sub> concentration is due to secondary pollution.

and Meng, 2022).

Pollution dispersal models can be used to address this issue (Ash and Fetter, 2004; Morello-Frosch and Jesdale, 2006; Muller and Mendelsohn, 2007; Sullivan, 2017; Cummiskey et al., 2019; Henneman et al., 2019). In recent years, a new generation of such models has emerged that not only account for atmospheric transport and chemical reactions - important for secondary pollution formation - but are also available at fine spatial scales with relative computational tractability. In particular, one such product, InMAP, has enabled source-attribution analyses of pollution disparities at resolutions down to 1 km-by-1 km (Tessum, Hill and Marshall, 2017; Goodkind et al., 2019; Tessum et al., 2019, 2021). Like Thind et al. (2019), our analysis uses InMAP to understand the air pollution disparity consequences of the U.S. electricity sector. However, in contrast to Thind et al. (2019)'s static analysis, we use panel emissions and demographic data to explore trends in these pollution disparities and then decompose these trends into their various drivers.

Our decomposition of pollution disparity trends builds on a long tradition in environmental and energy economics (Leontief, 1970; Selden, Forrest and Lockhart, 1999; Metcalf, 2008). Such techniques have been applied to understanding the determinants of pollution using data at various sectoral levels, with recent analyses conducted at the 4-digit Standard Industrial Classifications and product levels (Levinson, 2009; Shapiro and Walker, 2018). Our decomposition exercise extends this literature in three ways. First, we conduct a decomposition at the facility level, that is at the locations where pollution is emitted. This is critical since quantifying changes in pollution disparities requires knowing how the spatial distribution of emissions has evolved over time. Second, our decomposition examines composition changes in inputs and not just of outputs. A focus on input shares helps to explore the role played by recent coal-to-natural gas fuel switching in U.S. electricity generation. Third, our use of a pollution dispersal model together with data on the changing spatial pattern of demographic characteristics allows us to further characterize the role played by residential sorting in altering pollution disparities.

The remainder of the paper is organized as follows. Section 2 discusses our data. Section 3 details our methods. Section 4 presents our results. Section 5 concludes.

## 2 Data

Our analysis involves three main datasets: 1) emissions from electricity generating units (EGUs) in the continental United States, 2) smoke stack characteristics for EGUs, and 3) socioeconomic characteristics at the census-tract level.

## 2.1 Electricity generating units data

Electricity production and emissions data come from the U.S. Environmental Protection Agency's Clean Air Markets Division (EPA CAMD), which maintains data collected from the Continuous Emissions Monitoring Systems (CEMS) installed on EGUs over 25MW in capacity size (EPA, 2022a). The data includes hourly production quantities, fuel inputs, and hourly CO<sub>2</sub>, NO<sub>x</sub> and SO<sub>2</sub> emissions at the EGU level. We sum hourly observations to obtain total annual emissions for each EGU over 2000-2018 period.<sup>5</sup> A second EPA CAMD dataset provides facility-level latitude, longitude, and fuel type (EPA, 2022b), which we link at the EGU level to the CEMS data using power plant (ORISPL code) and EGU identifiers.<sup>6</sup> Our sample includes 4328 EGUs, corresponding to 1744 unique power plants.<sup>7</sup>

We merge CEMS data with smoke stack characteristics, obtained from the EIA Form 860. These data include stack height, temperature, velocity, and diameter, all of which are important for determining how far pollution travels upon leaving the smoke stack. Stack characteristics are available for 2007, 2008, 2009, and 2011; we match these characteristics to the generating units for the closest year available. As EIA data are at the smoke stack and not EGU level, a single EGU might be associated with multiple stacks, while a single stack might be shared among multiple EGUs. When an EGU is associated with multiple stacks, we divide emissions evenly across the stacks. When a stack is associated with multiple EGUs, we aggregate EGUs emissions to the associated stack.<sup>8</sup>

Table A1 presents descriptive statistics for our EGU sample by input fuel in 2018. As expected, coal-fired EGUs have larger capacity and higher SO<sub>2</sub> and NO<sub>x</sub> emissions than EGUs using natural gas and oil. They also have smoke stacks that are higher and wider, which may cause pollution to be transported farther than shorter and narrower stacks.

---

<sup>5</sup>An EGU is a component of power plant, and one power plant may have multiple EGUs. Our unit of analysis is at the EGU-level, not power plant-level, as EGUs within a powerplant may have different fuel and pollution smokestack characteristics, and thus unique emissions intensities and pollution transport patterns.

<sup>6</sup>The National Emissions Inventory is another database that EGU-level emissions and characteristics. However, it is only available for the years 2008, 2011, 2014, and 2017. For those years, the number of EGUs available from CEMs exceeds that from the NEI, which is why we use the CEMS data instead of the NEI data for our analysis.

<sup>7</sup>In the data analysis, we index units over time at the ORISPL-EGU-fuel level. By defining units by fuel, our decomposition analysis considers fuel switching of existing EGUs as part of compositional changes.

<sup>8</sup>On average per year, there are 109 EGUs with more than one stack associated and 1201 EGUs that share a stack.

## 2.2 Census-tract data

We use data on total population, Black share of population, Hispanic share of population, non-Hispanic White share of population, minority share of population,<sup>9</sup> and median income at the census-tract level. The 2000 data come from the Decennial Census while 2009-2018 data come from the American Community Survey (ACS, 5-year estimates).<sup>10</sup> Both were obtained from IPUMS NHGIS (Manson et al., 2021). The panels of Figure A1 shows each census tract's population share of individuals that identifies as Black, Hispanic, White and median income in 2018. Individuals from different racial/ethnic groups are not similarly distributed across the country: Black individuals tend to live in the southeastern and eastern states while Hispanic individuals are concentrated in the southwestern and western states. By contrast, income is relatively more evenly distributed across the country. This suggests that changes in electricity sector pollution concentrations could heterogeneously affect individuals from different racial/ethnic groups insofar as electricity generation is also spatially concentrated in certain regions.

## 2.3 Source-receptor matrix

To convert EGU-level primary  $\text{NO}_x$  and  $\text{SO}_2$  primary emissions to census-tract level secondary  $\text{PM}_{2.5}$  concentrations across the continental U.S., we use the InMAP input-source receptor matrix (SRM) developed by Goodkind et al. (2019). InMAP is a reduced-complexity chemical transport model that simulates  $\text{PM}_{2.5}$  concentrations from its precursor primary pollutants (Tessum, Hill and Marshall, 2017). We use the location and stack characteristics of our sample EGUs and InMAP's SRM to calculate total annual  $\text{PM}_{2.5}$  pollution concentrations in  $\mu\text{g}/\text{m}^3$  at the InMAP grid level.<sup>11</sup> We spatially aggregate the InMAP grid to the census tract level using census tract boundaries.<sup>12</sup> We do not use ambient  $\text{PM}_{2.5}$  measures (i.e. obtained from pollution monitors or satellite products) since such measures capture pollution from all sources whereas we are only interested in  $\text{PM}_{2.5}$  concentrations due to electricity generation.

---

<sup>9</sup>The minority share of population is the population share in a census tract who identify as Black or African American, Hispanic, Asian, American Indian and Alaska Native, or Native Hawaiian and Other Pacific Islander.

<sup>10</sup>This implies that we are missing census tract variables for the 2001-2008 period. Further, we do not use data from the 2010 Decennial Census to ensure consistency in our 2009-2018 measures, all obtained from the ACS.

<sup>11</sup>The InMAP grid level varies from 1 km up to 48 km depending on population density and uses year-invariant meteorological conditions from 2005.

<sup>12</sup>We use year-specific census tract shape files as census tract definitions change over time.

### 3 Methods

This section details our methods. Section 3.1 describes how we construct time trends in pollution concentrations from the U.S. electricity sector by demographic group. Section 3.2 discusses our decomposition of these trends.

#### 3.1 Trends in pollution concentrations by demographic groups

One common approach to understanding the forces driving pollution emissions is to represent facility-level emissions as a product of the overall (or national) scale of emissions, the composition of emissions across emitting facilities, and the emissions intensity (“technique”) of each facility.<sup>13</sup>

Let  $j$  index fossil-fuel electricity generating units (EGU). Our decomposition implies the following representation for year  $t$  emissions of pollutant  $p \in \{NO_x, SO_2\}$  from facility  $j$

$$E_{jt}^p = \phi_{jt}^p \delta_{jt} Q_t \quad (1)$$

where  $Q_t$  is national electricity output (in MWh), or the overall scale of US electricity production;  $\delta_{jt}$  is facility  $j$ ’s annual share of total electricity output, capturing the composition of emissions across facilities; and  $\phi_{jt}^p$  is each facility  $j$ ’s emissions intensity (in lbs per MWh). Note that since EGUs are defined by the fuel consumed, eq. (1) accommodates fuel switching within an EGU over time: an EGU that has switched fuels has  $\delta_{jt} = 0$  after the switch and is effectively treated as a new EGU with  $\delta_{jt} = 0$  before the switch. Entry of new EGUs and exit of existing EGUs are treated similarly: an EGU that exits production or has yet to enter into production has  $\delta_{jt} = 0$ .

We are interested in converting primary pollution emissions across facilities,  $E_{jt}^p$ , into secondary concentrations of PM<sub>2.5</sub> across locations. Let  $i$  index census tracts. For primary pollutant  $p$ ,  $\mathbf{W}^p$  is the InMAP source-receptor matrix (SRM), where element  $w_{ji}^p$  indicates the amount of secondary PM<sub>2.5</sub> pollution (in kg) received by census tract  $i$  from a 1 kg emission of primary pollutant  $p$  from facility  $j$ . Total secondary PM<sub>2.5</sub> concentration (in

---

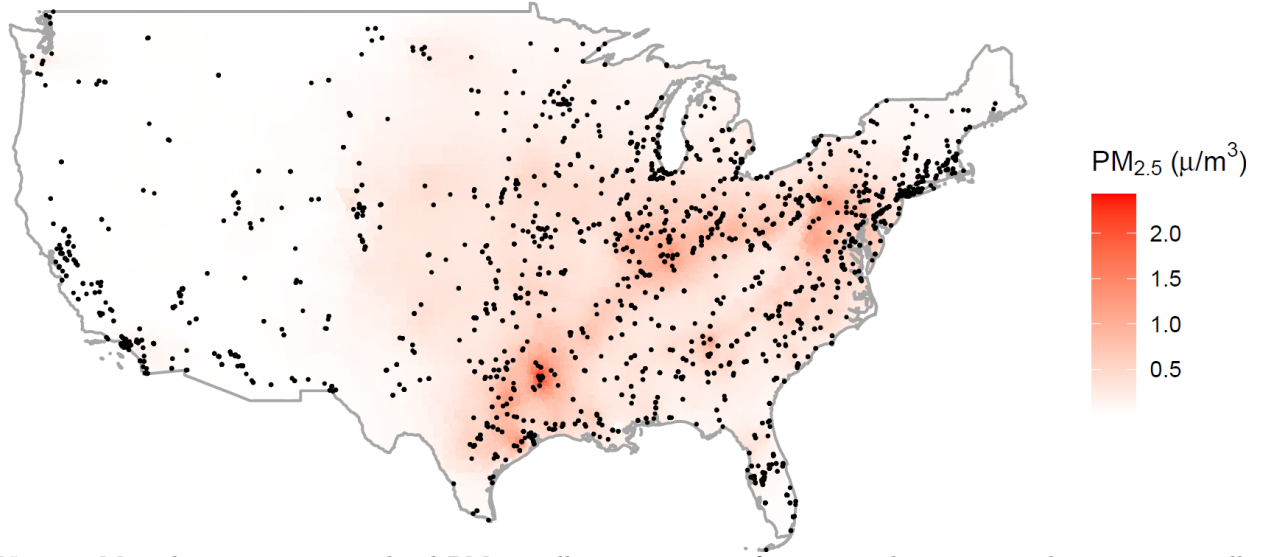
<sup>13</sup>This decomposition is also widely used in the environmental sciences literature. It is referred to as “I=PAT” when quantifying environmental impacts generally and as the Kaya Identity when applied to GHG emissions. The strength of this approach comes from decomposing pollution emissions into intuitive constituents that capture the overall scale of emissions in an economy, the composition of where emissions are coming from, and the technology behind these emissions. The main weakness of this approach is that it implicitly assumes these three drivers vary independently, which is unlikely. For example, a change in the pollution intensity of coal-fired electricity generation could alter the coal share of electricity, and possibly the overall pollution from electricity. Our decomposition approach, detailed in Section 3.2 allows for partial covariances between each incrementally added component. However, because we do not have exogenous variation in any of these components, causal interpretations are not possible.

$\mu/m^3$ ) in location  $i$  and year  $t$  is then the product of a facility's  $p$  emissions and its conversion PM<sub>2.5</sub> concentrations in location  $i$ , summed over all facilities and pollutants

$$C_{it} = \sum_p \sum_j E_{jt}^p w_{ji}^p \quad (2)$$

Figure 2 maps the PM<sub>2.5</sub> concentrations from all fossil fuel electricity production in 2018,  $C_{it}$ , as well as the location of each fossil fuel EGU. Figure A2 replicates Figure 2 but separately examining coal-, natural gas-, and oil-fired EGUs.

**Figure 2:** PM<sub>2.5</sub> concentrations from electricity generation



NOTES: Map shows census-tract level PM<sub>2.5</sub> pollution exposure from 2018 electricity production across all fossil fuel EGUs and the location of each fossil fuel EGU.

We next construct PM<sub>2.5</sub> concentrations from the electricity sector experienced by the average (continental) U.S. individual in demographic group  $g$ , where  $g$  may be a racial/ethnic group or income category. To do this, we must account for the uneven spatial distribution of individuals in group  $g$ , as shown in Figure A1. For example, because a greater share of the population in southeastern states comprise of Black individuals (see Figure A1b), one needs to weight PM<sub>2.5</sub> concentrations in that part of the country more so (using the local Black population) than in other regions when constructing a PM<sub>2.5</sub> concentration measure for the average Black individual. Specifically, we construct the following population-weighted pollution concentration for each demographic group  $g$  in year  $t$

$$C_{gt} = \frac{\sum_i C_{it} S_{git} N_{it}}{\sum_i S_{git} N_{it}} \quad (3)$$

where  $N_{it}$  is total population in census tract  $i$  during year  $t$  and  $S_{git}$  is the share of that

population in demographic group  $g$ . This is a population-weighted concentration measure because the product  $S_{git}N_{it}$  is the number of individuals in group  $g$  that live in census tract  $i$  in year  $t$ .<sup>14</sup> Combining these expressions, we have

$$C_{gt} = \frac{\sum_i \left( \sum_p \sum_j (\phi_{jt}^p \delta_{jt} Q_t) w_{ji}^p \right) S_{git} N_{it}}{\sum_i S_{git} N_{it}} \quad (4)$$

We examine trends in several pollution disparity measures, defined as differences in  $C_{gt}$  across groups. In particular, we explore the Black-White, Hispanic-White, and 1st-10th income decile pollution gaps.

### 3.2 Decomposing pollution concentration trends

Trends pollution disparities can be decomposed into various determinants. A standard exercise is to decompose changes in pollution emissions into changes due to the overall scale of electricity production, the pollution intensity of each EGU, and to the composition of electricity generation across EGUs, which includes fuel switching within EGUs and the entry and exit of EGUs. Our decomposition adds another component: changes in where individuals reside. Our decomposition exercise constructs variants of eq. (4), holding certain variables fixed to initial 2000 values.<sup>15</sup> Specifically, we consider the following set of scenarios:

**D1 Scale effect:** Fix  $\phi_{j,2000}^p, \delta_{j,2000}, S_{g,i,2000}, N_{i,2000}$ . Vary  $Q_t$ .

This scenario fixes emissions intensities, shares, and population distributions to their 2000 levels, while allowing the total quantity of electricity from total fossil fuels to change according to observed data. It isolates the change in pollution concentrations driven only by changes in the scale, or total quantity of fossil fuel electricity generation.

**D2 Scale + emissions intensity effects:** Fix  $\delta_{j,2000}, S_{g,i,2000}, N_{i,2000}$ . Vary  $Q_t$  and  $\phi_{jt}^p$ .

---

<sup>14</sup>For racial/ethnic groups, U.S. Census data provides annual data on the population share of a census tract belonging to each group, enabling the construction in eq. (3). For income, the U.S. Census provides median income at the census tract. Assuming that median income is uniformly distributed within a census tract, we define an indicator variable  $I_{dit}$  which equals one when census tract  $i$  has median income that falls in the  $d$ th decile of the year- $t$  income distribution across all U.S. census tracts. We then replace  $S_{git}$  with  $I_{dit}$  in eq. (3) to construct the PM<sub>2.5</sub> concentration experienced by the average individual in income decile  $d$  in year  $t$ .

<sup>15</sup>Alternatively, one could write eq. (4) in vector notation and apply a total derivative. The sum of each component could then recover the total change in pollution. The total derivative is a local linear approximation, which may not be appropriate for large changes. Our approach, which incrementally adds each component allows us to capture any potential covariances between components.

This scenario adds to D1 by further allowing emissions intensities to vary according to observed data. It captures the change in pollution concentrations driven by scale and emissions intensity (or technique) effects.

**D3 Scale + emissions intensity + composition effects:** Fix  $S_{g,i,2000}$ ,  $N_{i,2000}$ . Vary  $Q_t$ ,  $\phi_{jt}^p$ , and  $\delta_{jt}$ .

This scenario adds to D2 by further allowing emissions shares to vary according to observed data. It captures the change in pollution concentrations driven by scale, emissions intensity, and compositional effects.

**D4 Total effect:** Vary  $Q_t$ ,  $\phi_{jt}^p$ ,  $\delta_{jt}$ ,  $S_{git}$ , and  $N_{it}$ .

This scenario adds to D3 by further allowing population distributions to vary according to observe data. It captures the change in pollution concentrations driven by scale, emissions intensity, compositional, and residential sorting effects.<sup>16</sup>

## 4 Results

Section 4.1 details recent 2018 spatial patterns of PM<sub>2.5</sub> concentration from electricity across demographic groups. Section 4.2 presents 2000-2018 trends in PM<sub>2.5</sub> concentrations for each demographic group. Section 4.3 shows trends in PM<sub>2.5</sub> disparities and decomposes these trends. Section 4.4 offers additional evidence of a potential underlying mechanism.

### 4.1 Current spatial patterns of pollution concentrations

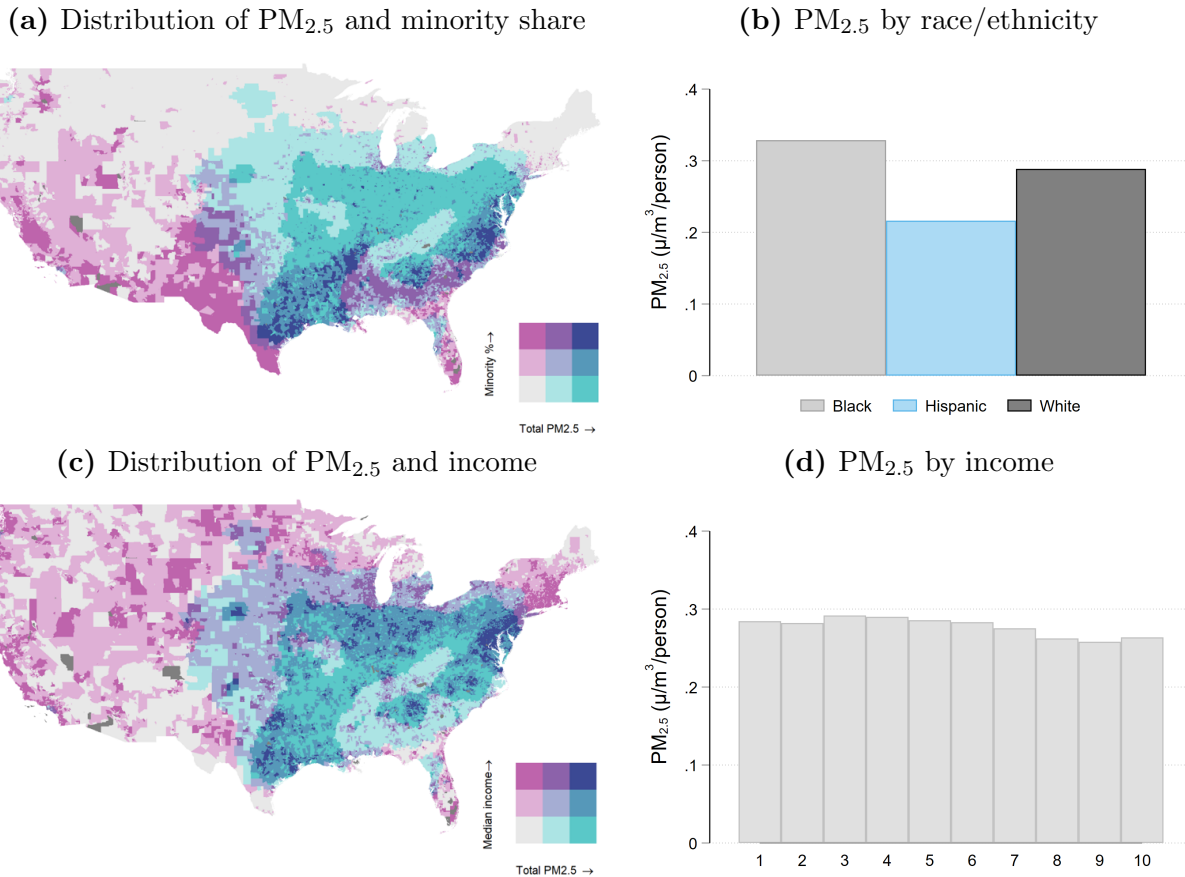
We begin by presenting spatial patterns of PM<sub>2.5</sub> from electricity in relation to where individuals of different demographic groups reside for 2018, the most recent year of our data. Figure 3a overlays PM<sub>2.5</sub> concentrations (in  $\mu\text{g}/\text{m}^3$ ) and minority share of population for each census tract in 2018. Because PM<sub>2.5</sub> from electricity is unevenly distributed across the country and because Black, Hispanic, and White individuals tend to reside in different regions, PM<sub>2.5</sub> concentrations differ for the average Black, Hispanic, and White individual, as shown in Figure 3b. PM<sub>2.5</sub> concentrations are highest for the average Black individual, followed by White, and Hispanic. This gap is large: the average Black individual is exposed to 64% more PM<sub>2.5</sub> from electricity than the average Hispanic individual. This ordering reflects

---

<sup>16</sup>We are unable to construct PM<sub>2.5</sub> concentrations for this scenario for the years 2001-2008 because census tract-level demographic variables  $S_{git}$  and  $N_{it}$  are not available from the ACS until 2009.

the joint spatial distribution of PM<sub>2.5</sub> concentrations and where individuals live. PM<sub>2.5</sub> concentrations from electricity are strongest across southern states where relatively more Black individuals live (Fig. A1a), followed by states in the midwest where relatively more White individuals live (Fig. A1c). There is far less PM<sub>2.5</sub> concentration in southwestern and western states where relatively more Hispanic individuals reside (Fig. A1b). By contrast, the income gradient is much smaller, as shown in Figure 3c-d. The average individual in the 1st income decile is exposed to 10% more PM<sub>2.5</sub> than the average individual in the 10th income decile. This is because in contrast to racial/ethnic dimensions, individual income is more evenly distributed across census tracts (Fig. A1d). Figures A3 and A4 break these patterns down for each fossil fuel.

**Figure 3:** PM<sub>2.5</sub> concentrations by demographic groups



**Notes:** Panel (a) overlays PM<sub>2.5</sub> concentrations from electricity generation and minority share of population for each census tract in 2018. Shading color-coded by terciles. Panel (b) shows the 2018 PM<sub>2.5</sub> concentrations for the average Black, Hispanic, and White individual, in  $\mu\text{m}^3/\text{person}$ . Panel (c) overlays PM<sub>2.5</sub> concentrations from electricity generation and median income for each census tract in 2018. Panel (d) shows the 2018 PM<sub>2.5</sub> concentrations for the average individual in each income decile, in  $\mu\text{m}^3/\text{person}$ .

## 4.2 Pollution concentration trends

Using time-varying data on EGU emissions and census-tract demographic characteristics, we calculate how PM<sub>2.5</sub> concentrations from electricity generation has evolved over 2000-2018 for each demographic group, or  $C_{gt}$ .

Figure 4a shows PM<sub>2.5</sub> concentrations for the average individual. Between 2000-2018, PM<sub>2.5</sub> concentrations fell by 87% or  $1.9 \mu/m^3/\text{person}$ .<sup>17</sup> To contextualize the magnitude of this fall in PM<sub>2.5</sub> concentrations from the electricity sector, the national average ambient PM<sub>2.5</sub> concentration from all pollution sources was  $13.5 \mu/m^3$  in 2000 and  $8.2 \mu/m^3$  in 2018, a drop of 39%.<sup>18</sup> The decline in PM<sub>2.5</sub> concentrations from electricity is more than double this rate. Or put another way, in 2000 PM<sub>2.5</sub> from the U.S. electricity sector was 16% of U.S. ambient PM<sub>2.5</sub> concentrations. In 2018, that percentage fell to 3.5%.

Figure 4b shows these PM<sub>2.5</sub> changes by racial/ethnic group. During this period, PM<sub>2.5</sub> concentrations decreased by 89%, 84%, and 87%, or  $2.6$ ,  $1.1$ , and  $1.9 \mu/m^3/\text{person}$ , for the average Black, Hispanic, and White individual, respectively. Given initial PM<sub>2.5</sub> concentration differences in 2000, these differential trends imply a dramatic convergence in pollution disparities across these racial/ethnic groups. While disparities still exist in 2018, they are much smaller than they were in 2000. Specifically, between 2000-2018, the observed Black-White PM<sub>2.5</sub> gap was consistently positive, with the average Black individual experiencing more PM<sub>2.5</sub> concentrations than the average White individual. But this gap fell from  $0.71$  to  $0.04 \mu/m^3/\text{person}$  between 2000-2018, or by 94%. At the same time, the Hispanic-White PM<sub>2.5</sub> disparity was consistently negative throughout our sample, with the average Hispanic individual experiencing less PM<sub>2.5</sub> concentration than the average White individual. However, as with the Black-White disparity, the Hispanic-White disparity has narrowed from  $-0.96$  to  $-0.08 \mu/m^3/\text{person}$  during 2000-2018, or 92% during this period.

Figure 4c plots PM<sub>2.5</sub> concentrations for the average individual in the bottom and top income deciles, which falls by 87% and 89%, or  $1.9$  and  $2.0 \mu/m^3/\text{person}$ , respectively. However, because of the smaller 2000 gap in PM<sub>2.5</sub> concentrations and the similarity of these trends, the PM<sub>2.5</sub> concentration gap between individuals in the bottom and top income deciles has been relatively unchanged during the 2000-2018 period. Figure A5 shows a similar pattern when comparing the average individual in the bottom and top quartiles.

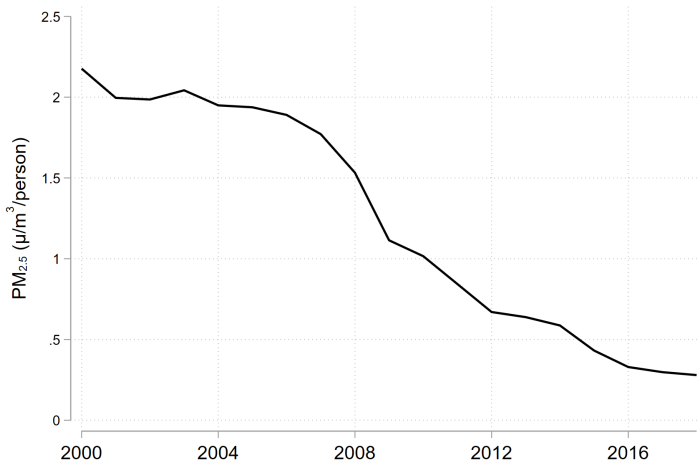
---

<sup>17</sup>PM<sub>2.5</sub> concentrations shown in Figure 4 hold demographic characteristics fixed to 2000 values (i.e., D3 in Section 3.2). This is because we are missing census tract-level demographics data for the years 2001-2008 prior to ACS availability, such that we are unable to construct actual PM<sub>2.5</sub> concentrations (i.e., D4 in Section 3.2) for those years. However, because residential locations have changed little between 2000-2018, the change in PM<sub>2.5</sub> concentration between 2000 and 2018 when applying 2000 demographic data to both years is nearly identical to that when applying 2000 and 2018 demographic data, as shown in Figure 6.

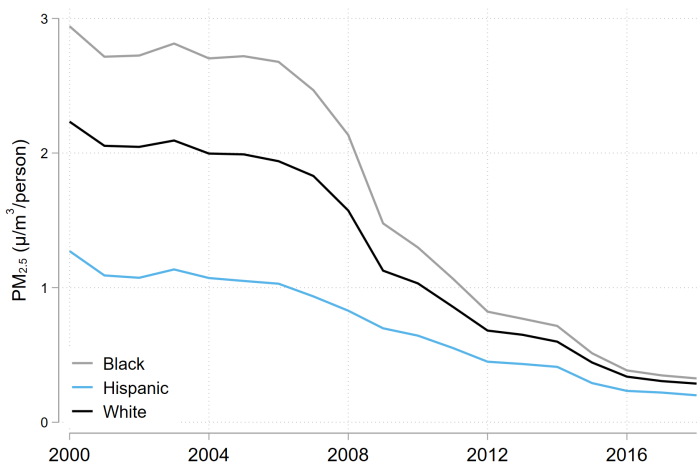
<sup>18</sup>Data available here: <https://www.epa.gov/air-trends/particulate-matter-pm25-trends>

**Figure 4:** Trends in pollution concentrations by demographics

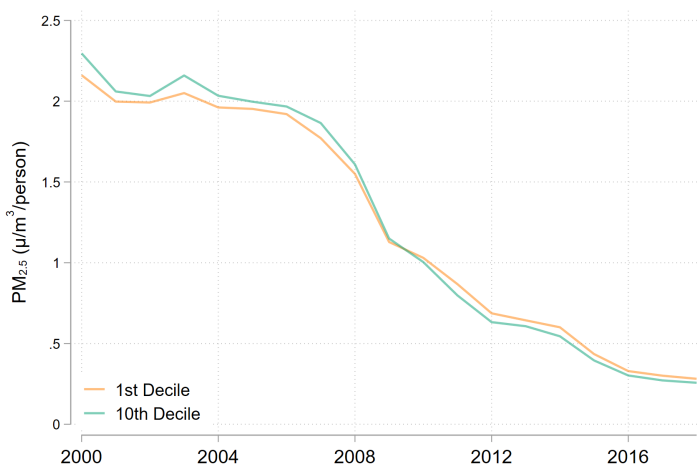
(a) Overall



(b) By race/ethnicity



(c) By income



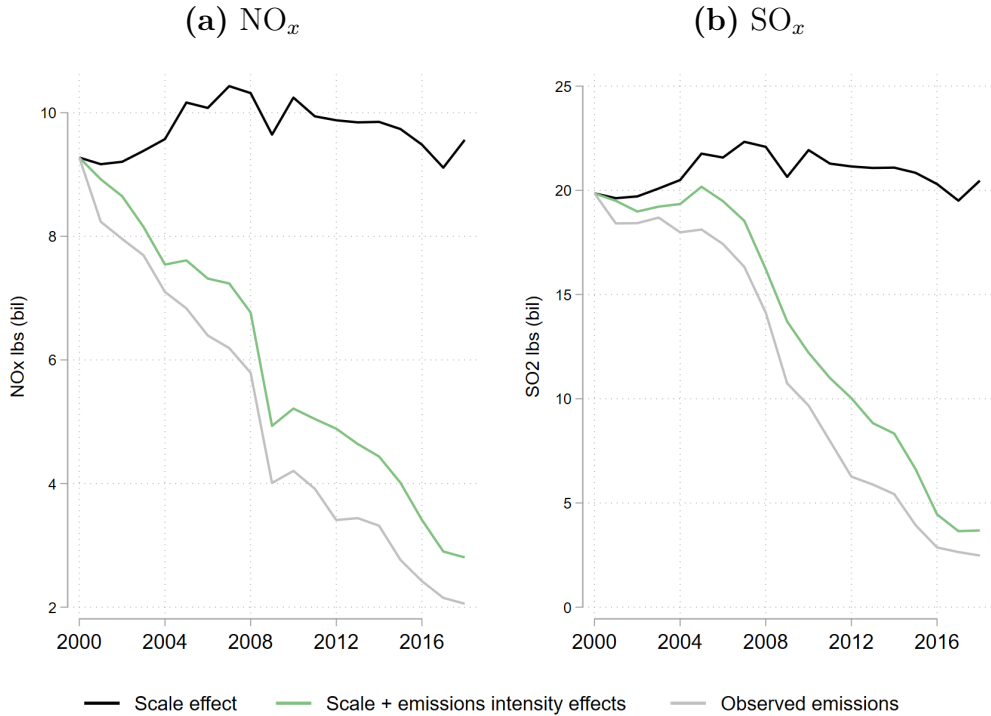
**Notes:** Panel (a) shows 2000-2018 PM<sub>2.5</sub> concentrations for the average U.S. individual. Panel (b) shows the average Black, Hispanic, and White individual. Panel (c) shows the average bottom and top income decile individual.

Given the presence of racial/ethnic PM<sub>2.5</sub> disparity trends and their absence along income differences, our subsequent decomposition will focus on racial/ethnic PM<sub>2.5</sub> disparities.

### 4.3 Decomposing pollution disparity trends

We conduct the decomposition scenarios described in Section 3.2 to explore the drivers behind the recent convergence in PM<sub>2.5</sub> disparities. Specifically, we decompose PM<sub>2.5</sub> disparity trends into changes in the scale of fossil fuel electricity generation, emissions intensities, the composition of EGUs, and where households of different racial/ethnic groups reside.

**Figure 5:** Decomposition of NO<sub>x</sub> and SO<sub>2</sub> emissions trends



**Notes:** Panel (a) shows the decomposition of primary NO<sub>x</sub> emissions (in billion lbs). Panel (b) shows for primary SO<sub>2</sub> emissions (in billion lbs).

We begin with Figure 5, which, much like Levinson (2009) and Shapiro and Walker (2018) shows how emissions changes can be decomposed into scale, emissions intensity, and compositional changes. Panel (a) shows NO<sub>x</sub> emissions while panel (b) shows SO<sub>2</sub> emissions. Overall emissions have fallen dramatically: between 2000-2018, emissions fell by 78% and 88% for NO<sub>x</sub> and SO<sub>x</sub>, respectively (gray series). For both pollutants, the scale effect alone contributes a modest 4% of overall emission changes (black series). Note that as renewables are not included here, these scale effects can be thought of as the scale effects of fossil generation, e.g. changes in output satisfying residual demand met by fossil generation,

total demand less renewables. By contrast, 86% and 89% of emissions reductions can be attributed to emissions intensity changes for  $\text{NO}_x$  and  $\text{SO}_x$ , respectively (green minus black series). Compositional changes contribute the remaining 10% and 7% for  $\text{NO}_x$  and  $\text{SO}_x$ , respectively (gray minus green series).

The decomposition of emissions serve as an input into our decomposition of  $\text{PM}_{2.5}$  disparity trends. Figure 6a shows the Black-White  $\text{PM}_{2.5}$  concentrations difference decomposed into scale, emissions intensity, compositional, and residential sorting components. Changes in emission intensities is by far the largest driver, contributing 93% of the overall change in the Black-White  $\text{PM}_{2.5}$  disparity (green minus black series). By contrast, scale (black series) and compositional (gray minus green series) effects contributed only 2% and 6%, respectively. Changes in residential location had a negligible effect (blue minus gray series). Similarly, an overwhelming share of the Hispanic-White  $\text{PM}_{2.5}$  disparity can be explained by changes in emissions intensities alone. Compositional changes, such as fuel switching, and residential location changes explain much less.<sup>19</sup>

## 4.4 Mechanism

Why might changes in emissions intensities play such a large role in reducing  $\text{PM}_{2.5}$  disparities? Recall that to alter pollution disparities, it matters where emissions intensity improvements are occurring. In particular, it depends on whether improvements are occurring from EGUs that are upwind of disadvantaged individuals. This section provides additional evidence on such patterns.

To understand the spatial relationship between where emissions intensity improvements are occurring for coal-fired EGUs and who is downwind of these improvements, we construct county-average emissions intensities from coal-fired EGUs separately for  $\text{NO}_x$  and  $\text{SO}_2$  in each year of the study period. We measure improvement as the difference between county-average emissions intensity in 2018 compared to 2000.<sup>20</sup> We bin counties into vigintiles (i.e., 20 bins) according to pollutant-specific emissions intensity improvements, where bin 20 indicates the largest emissions intensity improvements. Within each pollutant-bin, we feed a common pulse of emission for all coal-fired EGUs into InMap, which enables us to examine the differential downwind impacts separate from the scale of emissions from each EGU.<sup>21</sup>

Figure 7 shows these pollution intensity bins on the horizontal axis. The vertical axis shows the resulting secondary  $\text{PM}_{2.5}$ -weighted Black population affected from the uniform

---

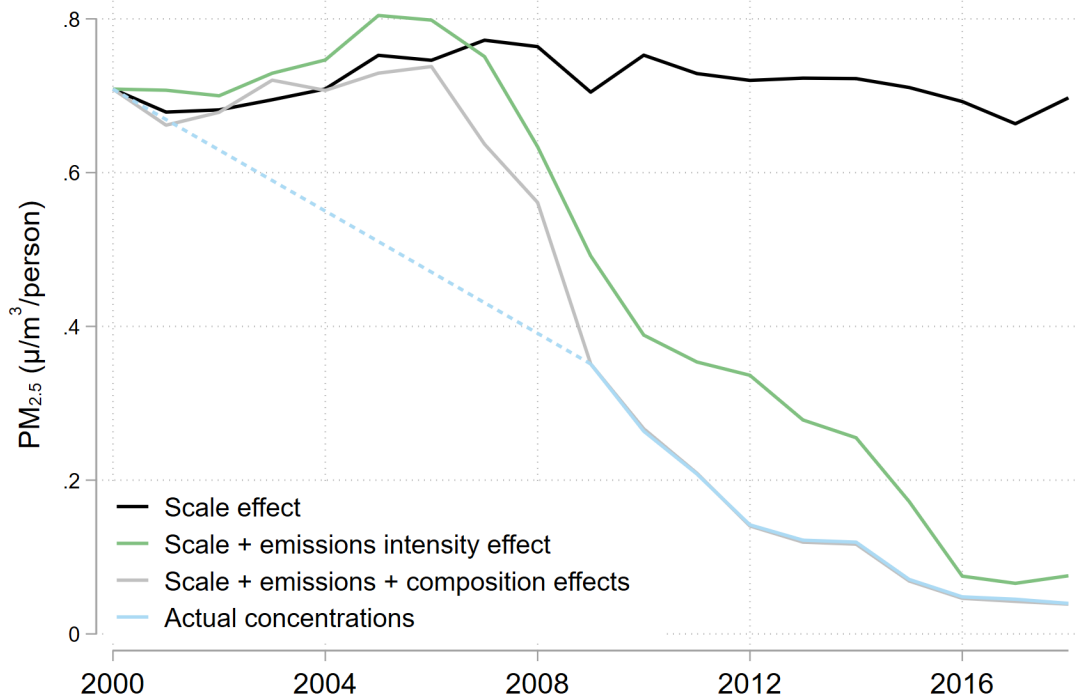
<sup>19</sup>Figures A6-A8 replicate Figure 6 for each fossil fuel.

<sup>20</sup>We look at county-average improvements instead of EGU-specific improvements as we want to capture both within EGU improvement and improvements generated by the entry and exit of EGUs.

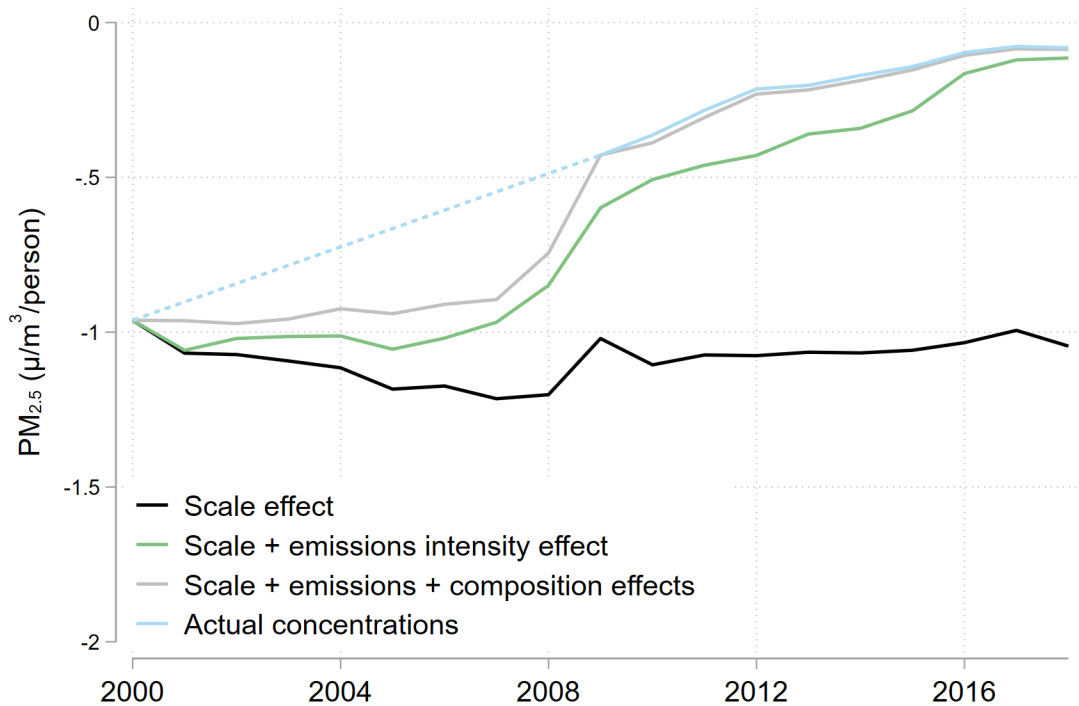
<sup>21</sup>With 20 bins and 2 pollutants, this leads to 40 unique InMap runs. Within each run, we assign a 10,000 kg pulse of pollution for each coal-fired EGU.

**Figure 6:** Decomposition of pollution disparity trends

(a) Black-White disparity

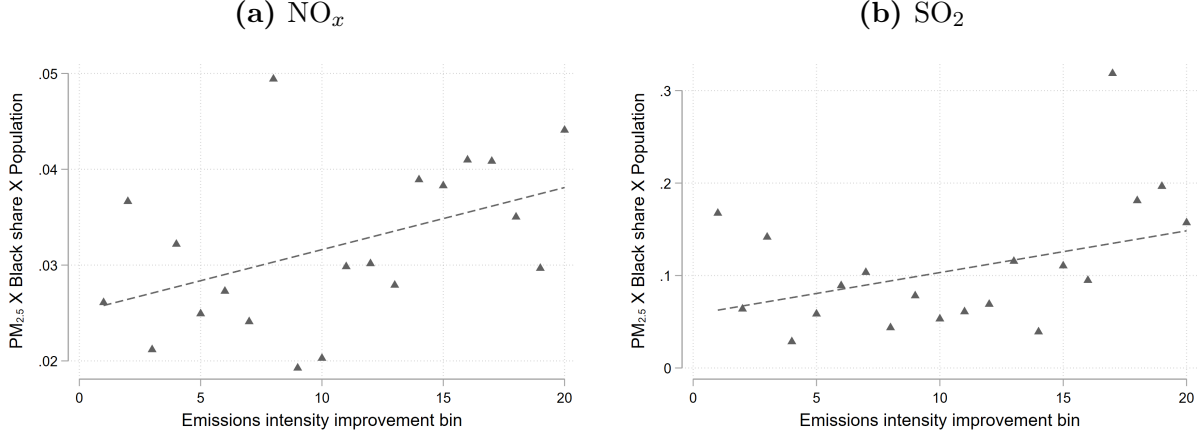


(b) Hispanic-White disparity



**Notes:** Panel (a) shows the Black-White PM<sub>2.5</sub> disparity trend and its components over 2000-2018. Panel (b) shows the Hispanic-White PM<sub>2.5</sub> disparity trend and its component over 2000-2018. Dashed line shows interpolated value during 2001-2008 in the absence of census tract-level demographic data.

**Figure 7:** Correlation between emissions intensity improvements and affected Black population



**Notes:** Panel (a) shows the relationship between the emissions intensity improvement bins and the resulting secondary PM<sub>2.5</sub>-weighted Black population affected by a unit increase in primary NO<sub>x</sub> emissions. Panel (b) examines primary SO<sub>x</sub> emissions.

pulse of primary NO<sub>x</sub> in panel (a) and SO<sub>x</sub> in panel (b). The positive relationships in Figure 7 indicate that counties that experienced greater improvements in emissions intensities from coal-fired EGUs are also upwind of more Black individuals.

## 5 Conclusion

Electricity generation is a major source of U.S. pollution, with resulting PM<sub>2.5</sub> concentrations that are unevenly distributed across demographic groups. To address this, attention has been increasingly paid to understanding the pollution disparity consequences of various policies. This paper quantifies 2000-2018 trends in PM<sub>2.5</sub> disparities arising from the US electricity sector through the use of a high spatial resolution pollution transport model. Our analysis reveals several new findings with policy implications.

We find that between 2000-2018, PM<sub>2.5</sub> concentrations have fallen by 87% for the average individual, which is more than double the decline rate in overall U.S. ambient PM<sub>2.5</sub> concentrations over the same period. Moreover, this decline is broadly shared across racial/ethnic groups: we detect a 89%, 87%, and 84% PM<sub>2.5</sub> decline for the average Black, Hispanic, White individual, respectively. But because 2000 PM<sub>2.5</sub> concentration levels are highest for Black, followed by White and Hispanic individuals, these trends imply a dramatic convergence in PM<sub>2.5</sub> concentrations across these racial/ethnic groups. Specifically, the Black-White PM<sub>2.5</sub> disparity, while consistently positive during this period has narrowed (or fallen) by 94% since 2000. During this period, the Hispanic-White PM<sub>2.5</sub> disparity, which is consistently

negative, has narrowed (or risen) by 92%. However, we note that despite this convergence, racial-ethnic PM<sub>2.5</sub> disparities from electricity still exist in 2018. Interestingly, while the PM<sub>2.5</sub> concentration for the average bottom and top income decile individual fell by 87% and 89%, respectively, the gap between low and high income individuals has been relatively small and largely unchanged during this period. These differential patterns indicate that what happens to one demographic group need not apply to another, reflecting the need for policies that acknowledge how pollution concentrations and their trends differ across demographic groups.

Our decomposition exercise reveals that nearly all of these disparity trends can be attributed to spatially-varying improvements in emissions intensities. By contrast, compositional changes, which incorporates recent coal-to-natural gas fuel switching, and changes in residential location contributed much less. Emissions intensity changes are often associated with local air pollution policies, such as the Clean Air Act, suggesting that such policies can play an important role in further reducing pollution disparities from the U.S. electricity sector moving forward.

Our finding that compositional changes among fossil fuel generators contributed little to changing pollution disparities need not imply similar impacts for future US climate policy. A likely consequence of any climate policy is the expansion of renewable sources of electricity, which does not emit air pollution. Future research should consider how expansion of renewable energy differentially replaces coal, oil, and natural gas generation and where.

A more complete analysis would also consider the efficiency consequences of changing electricity prices and any added distributional effects related to the incidence of such price changes across demographic groups. This would enable an exploration of equity-efficiency trade-offs across a variety of proposed environmental and climate policies. For example, suppose policy makers face the joint objectives of achieving a GHG target in a cost-effective manner and narrowing existing local air pollution disparities. This can be implemented by combining a carbon price with a regulation targeting polluters that disproportionately affect disadvantaged individuals. If cost-effective GHG abatement across facilities coincides with declines in pollution disparities, there would be no trade-off. However, if cost-effective abatement also increases pollution disparities, policy makers must now weight higher electricity prices (and its distributional impacts) against narrowing pollution disparities when considering the ideal mix of policies. Characterizing where these trade-offs exists and how they can be navigated through policy design can inform environmental and climate policies that jointly advance environmental, cost-effectiveness, and equity goals.

## References

- Ash, Michael, and T. Robert Fetter. 2004. "Who Lives on the Wrong Side of the Environmental Tracks? Evidence from the EPA's Risk-Screening Environmental Indicators Model." *Social Science Quarterly*, 85(2): 441–462.
- Banzhaf, Spencer, Lala Ma, and Christopher Timmins. 2019. "Environmental Justice: The Economics of Race, Place, and Pollution." *Journal of Economic Perspectives*, 33(1): 185–208.
- Bowen, William. 2002. "An Analytical Review of Environmental Justice Research: What do we Really Know?" *Environmental Management*, 29(1): 3–15.
- Bullard, Robert. 2000. *Dumping in Dixie: Race, Class, and Environmental Quality*. Westview Press.
- Colmer, Jonathan, Ian Hardman, Jay Shimshack, and John Voorheis. 2020. "Disparities in PM2.5 air pollution in the United States." *Science*, 369(6503): 575–578.
- Cummiskey, Kevin, Chanmin Kim, Christine Choirat, Lucas R. F. Henneman, Joel Schwartz, and Corwin Zigler. 2019. "A Source-Oriented Approach to Coal Power Plant Emissions Health Effects."
- Currie, Janet, John Voorheis, and Reed Walker. 2021. "What Caused Racial Disparities in Particulate Exposure to Fall? New Evidence from the Clean Air Act and Satellite-Based Measures of Air Quality." National Bureau of Economic Research Working Paper 26659.
- Deschenes, Olivier, and Kyle C Meng. 2018. "Quasi-experimental Methods in Environmental Economics: Challenges and Opportunities." *Handbook of Environmental Economics*, 4: 285.
- EPA, United States Environmental Protection Agency. 2022a. "Power Sector Emissions Data."
- EPA, United States Environmental Protection Agency. 2022b. "Power Sector Facility Attributes Data."
- EPA, US. 2018. "2014 National Emissions Inventory (NEI) Data."
- Goodkind, Andrew L, Christopher W Tessum, Jay S Coggins, Jason D Hill, and Julian D Marshall. 2019. "Fine-scale damage estimates of particulate matter air pollution reveal

- opportunities for location-specific mitigation of emissions.” *Proceedings of the National Academy of Sciences*, 116(18): 8775–8780.
- Henneman, Lucas R.F., Christine Choirat, Cesunica E. Ivey, Kevin Cummiskey, and Corwin M. Zigler. 2019. “Characterizing population exposure to coal emissions sources in the United States using the HyADS model.” *Atmospheric Environment*, 203(203): 271–280.
- Hernandez-Cortes, Danae, and Kyle C Meng. 2022. “Do Environmental Markets Cause Environmental Injustice? Evidence from California’s Carbon Market.” National Bureau of Economic Research Working Paper 27205.
- Leontief, Wassily. 1970. “Environmental repercussions and the economic structure: an input-output approach.” *The review of economics and statistics*, 262–271.
- Levinson, Arik. 2009. “Technology, international trade, and pollution from US manufacturing.” *American economic review*, 99(5): 2177–92.
- Manson, Steven, Jonathan Schroeder, David Van Riper, Tracy Kugler, and Steven Ruggles. 2021. “IPUMS National Historical Geographic Information System: Version 16.0.” *[dataset]*. Minneapolis, MN: IPUMS.
- Metcalf, Gilbert E. 2008. “An empirical analysis of energy intensity and its determinants at the state level.” *The Energy Journal*, 29(3).
- Mohai, Paul, David Pellow, and J. Timmons Roberts. 2009. “Environmental Justice.” *Annual Review of Environment and Resources*, 34(1): 405–430.
- Morello-Frosch, Rachel, and Bill M Jesdale. 2006. “Separate and Unequal: Residential Segregation and Estimated Cancer Risks Associated with Ambient Air Toxics in US Metropolitan Areas.” *Environmental Health Perspectives*, 114(3): 386.
- Muller, Nicholas Z, and Robert Mendelsohn. 2007. “Measuring the damages of air pollution in the United States.” *Journal of Environmental Economics and Management*, 54(1): 1–14.
- Ringquist, Evan J. 2005. “Assessing Evidence of Environmental Inequities: A Meta-analysis.” *Journal of Policy Analysis and Management*, 24(2): 223–247.
- Selden, Thomas M, Anne S Forrest, and James E Lockhart. 1999. “Analyzing the reductions in US air pollution emissions: 1970 to 1990.” *Land Economics*, 1–21.

Shapiro, Joseph S, and Reed Walker. 2018. "Why is pollution from US manufacturing declining? The roles of environmental regulation, productivity, and trade." *American Economic Review*, 108(12): 3814–54.

Sullivan, Daniel M. 2017. "The True Cost of Air Pollution: Evidence from the Housing Market." *mimeo*.

Tessum, Christopher W, David A Paolella, Sarah E Chambliss, Joshua S Apte, Jason D Hill, and Julian D Marshall. 2021. "PM2.5 polluters disproportionately and systemically affect people of color in the United States." *Science Advances*, 7(18): eabf4491.

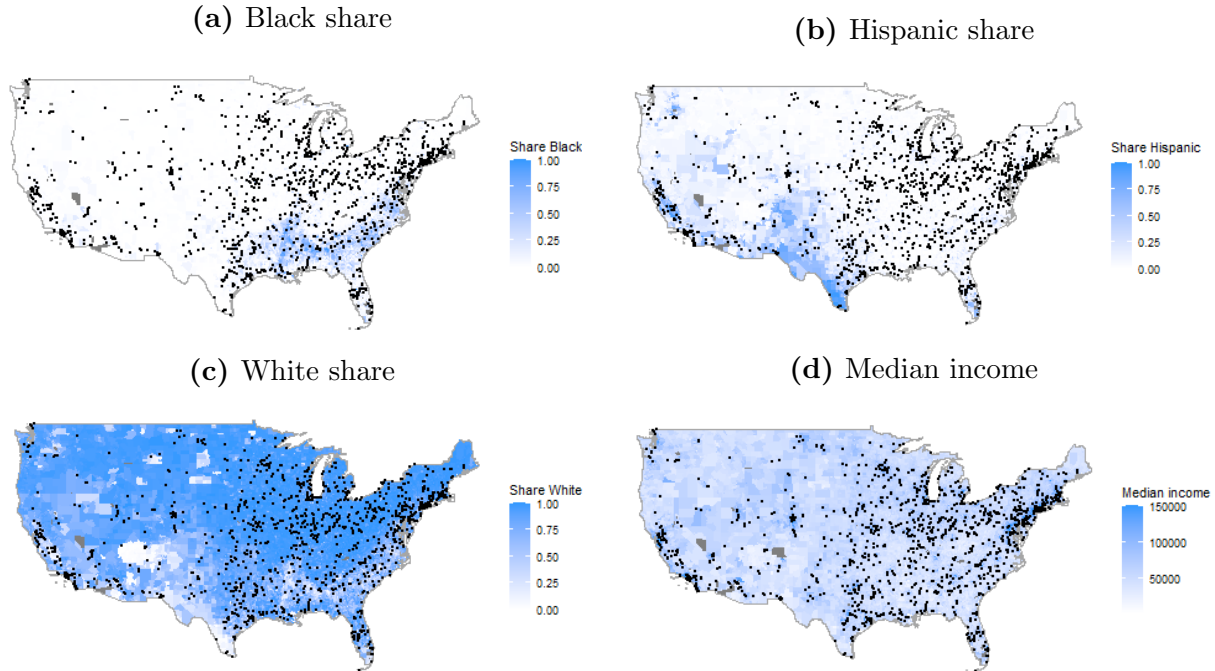
Tessum, Christopher W., Jason D. Hill, and Julian D. Marshall. 2017. "InMAP: A model for air pollution interventions." *PLOS ONE*, 12(4): 1–26.

Tessum, Christopher W., Joshua S. Apte, Andrew L. Goodkind, Nicholas Z. Muller, Kimberley A. Mullins, David A. Paolella, Stephen Polasky, Nathaniel P. Springer, Sumil K. Thakrar, Julian D. Marshall, and Jason D. Hill. 2019. "Inequity in consumption of goods and services adds to racial–ethnic disparities in air pollution exposure." *Proceedings of the National Academy of Sciences*, 116(13): 6001–6006.

Thind, Maninder PS, Christopher W Tessum, Inês L Azevedo, and Julian D Marshall. 2019. "Fine particulate air pollution from electricity generation in the US: Health impacts by race, income, and geography." *Environmental Science & Technology*, 53(23): 14010–14019.

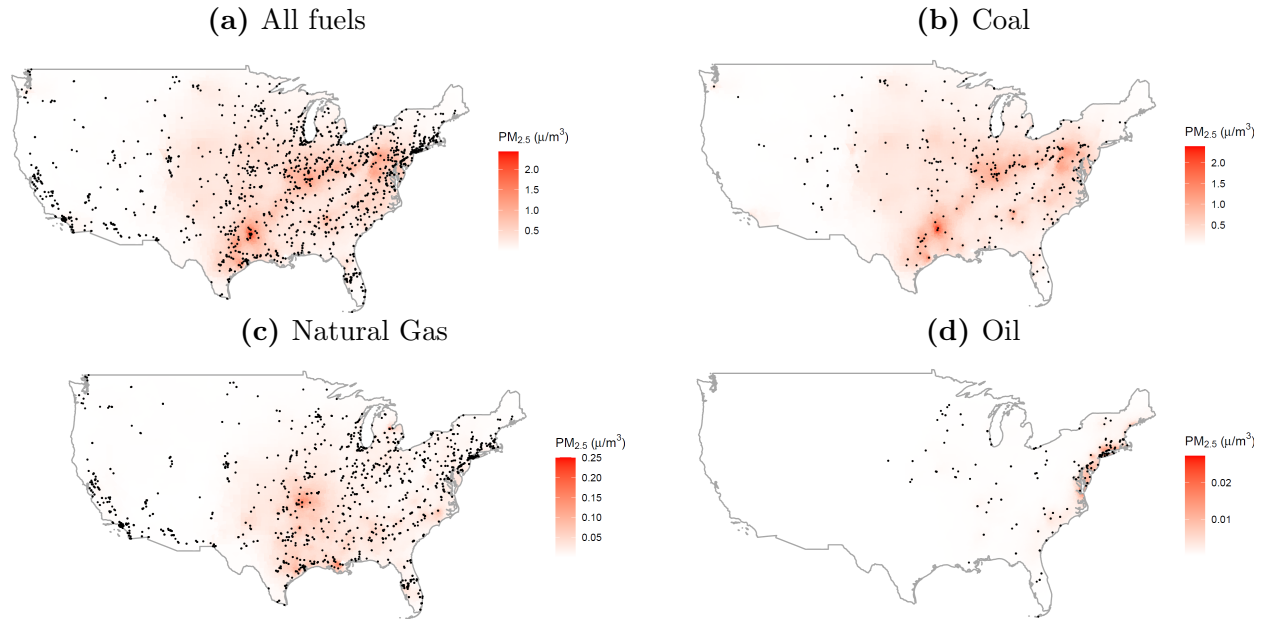
## Appendix A: Additional Figures

**Figure A1:** Census tract racial/ethnic population shares and median income in 2018



**Notes:** Panel (a) shows the Black population share at the census tract level. Panel (b) shows the Hispanic population share. Panel (c) shows the White population share. Panel (d) shows household median income. Points denote the location of all fossil fuel EGUs.

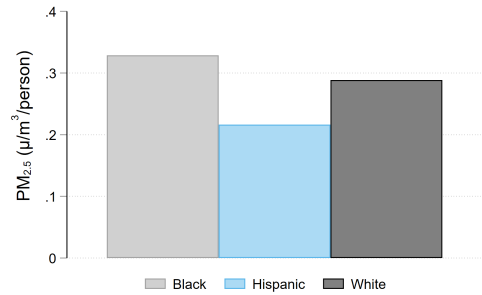
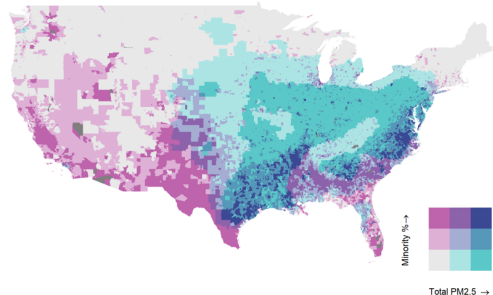
**Figure A2:** PM<sub>2.5</sub> concentrations from electricity generation by fuel



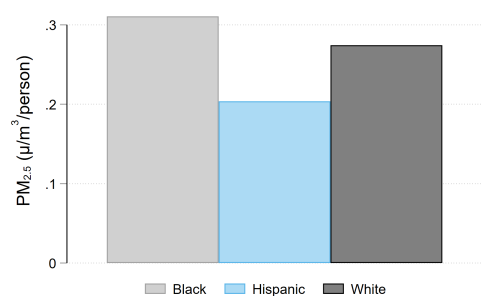
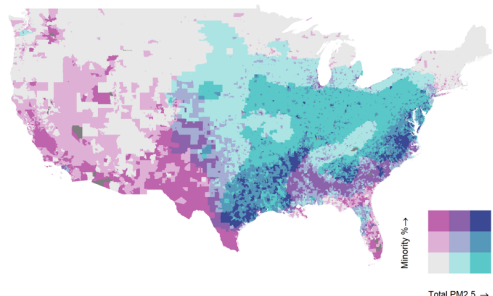
NOTES: Panel (a) shows PM<sub>2.5</sub> pollution exposure from 2018 electricity generation from all fossil fuel EGUs at the census tract level. Points denote the location of all fossil fuel EGUs. Panels (b), (c), and (d) show for coal-, natural gas-, and oil-fired EGUs only, respectively.

**Figure A3:** PM<sub>2.5</sub> concentrations by racial/ethnic groups and fuel

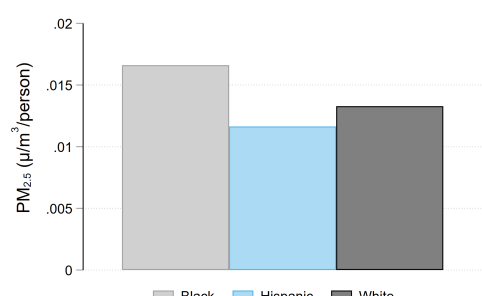
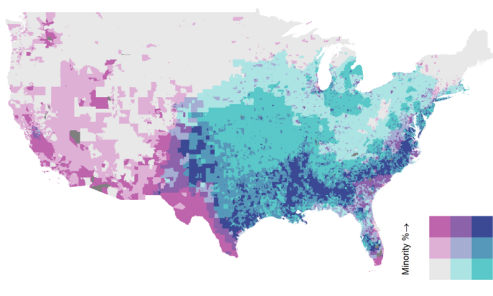
(a) All fuels



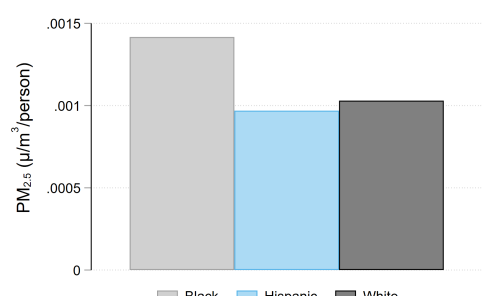
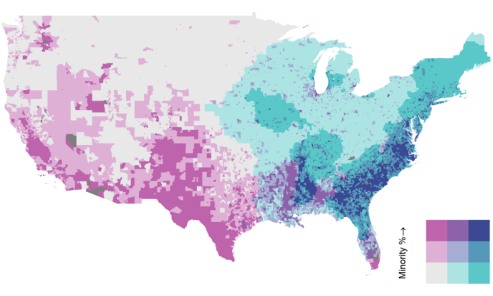
(b) Coal



(c) Natural Gas

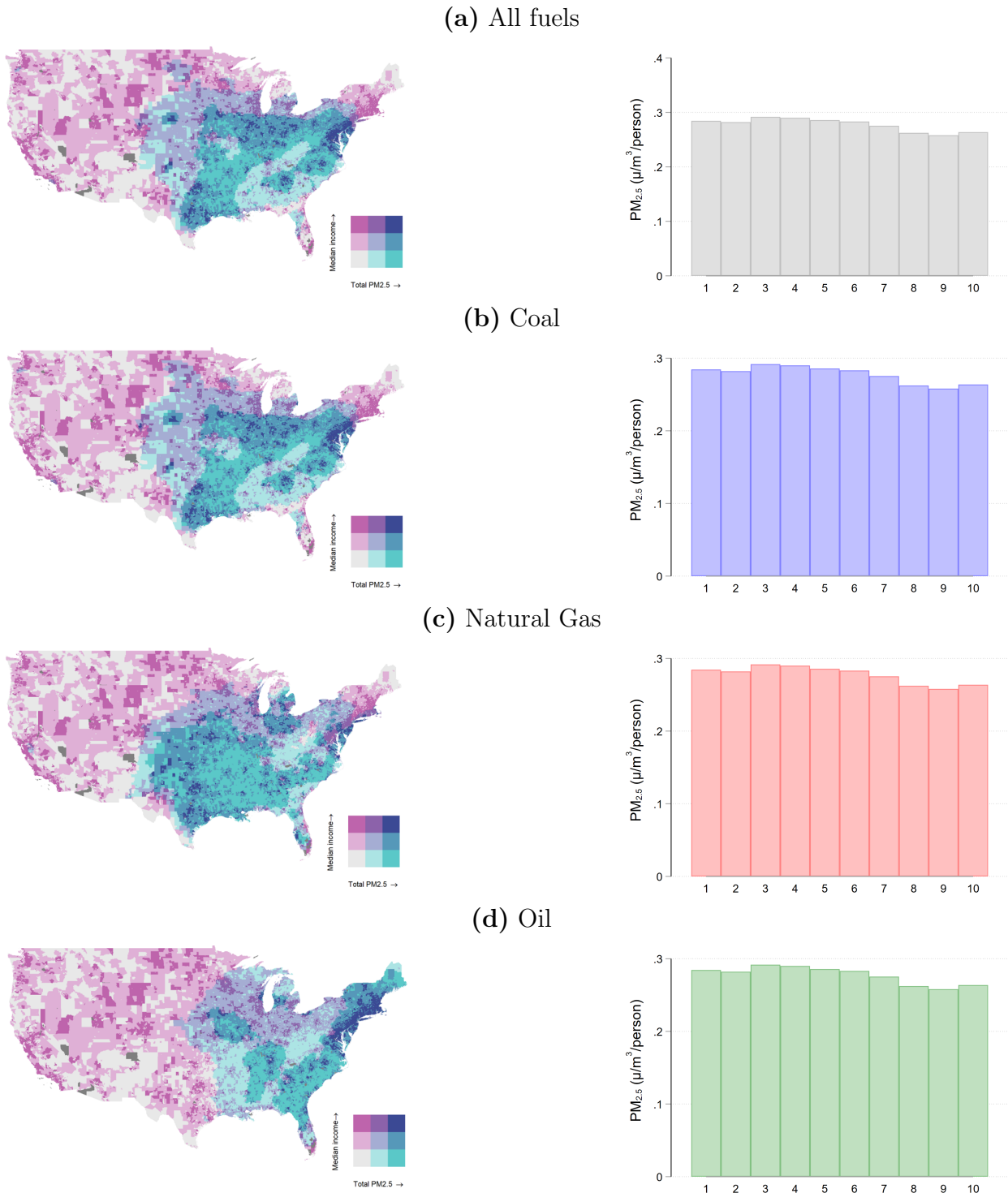


(d) Oil



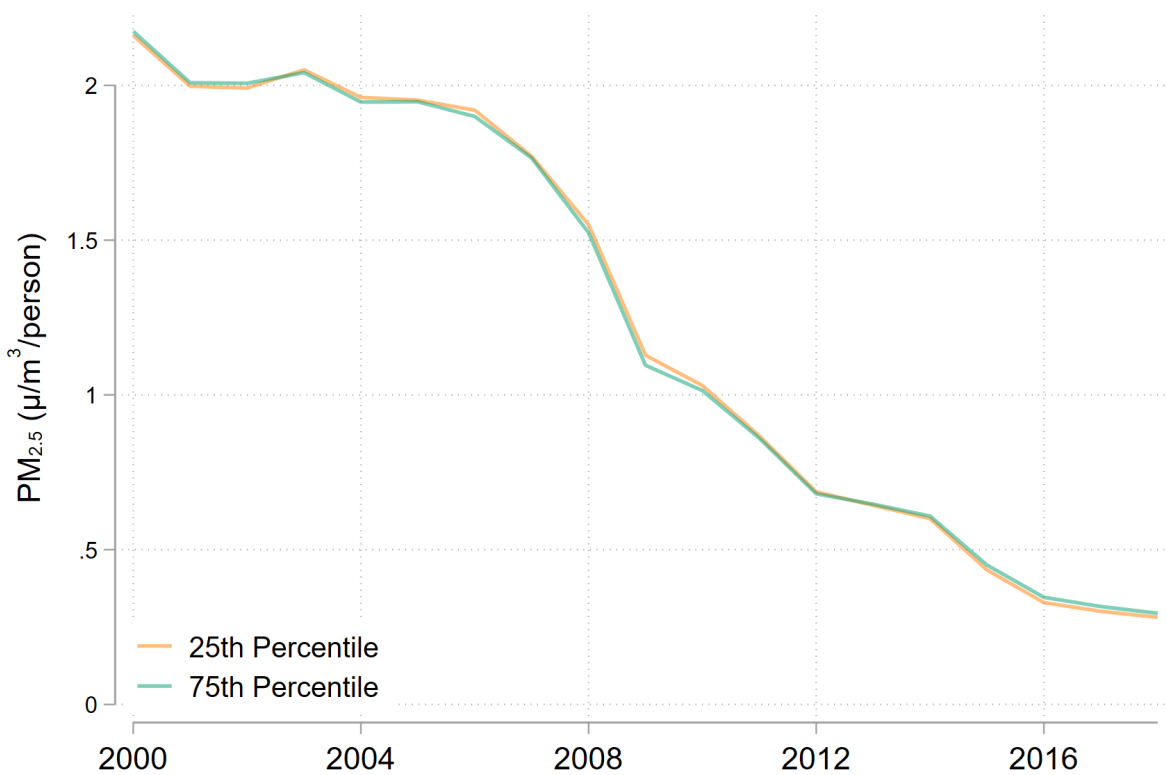
**Notes:** Left column overlays PM<sub>2.5</sub> concentration from electricity production and minority share of population for each census tract in 2018. Shading color-coded by terciles. Right column shows the PM<sub>2.5</sub> concentration for the average White, Black, and Hispanic individual, in  $\mu/m^3/person$ . Panel (a) uses all fossil fuel-fired EGUs, while Panels (b), (c), and (d) uses coal-, natural gas-, and oil-fired EGUs only, respectively.

**Figure A4:** PM<sub>2.5</sub> concentrations by income and fuel



**Notes:** Left column overlays PM<sub>2.5</sub> concentration from electricity production and median income for each census tract in 2018. Shading color-coded by terciles. Right column shows the PM<sub>2.5</sub> concentration for the average individual in each income decile, in  $\mu\text{m}^3/\text{person}$ . Panel (a) uses all fossil fuel-fired EGUs, while Panels (b), (c), and (d) uses coal-, natural gas-, and oil-fired EGUs only, respectively.

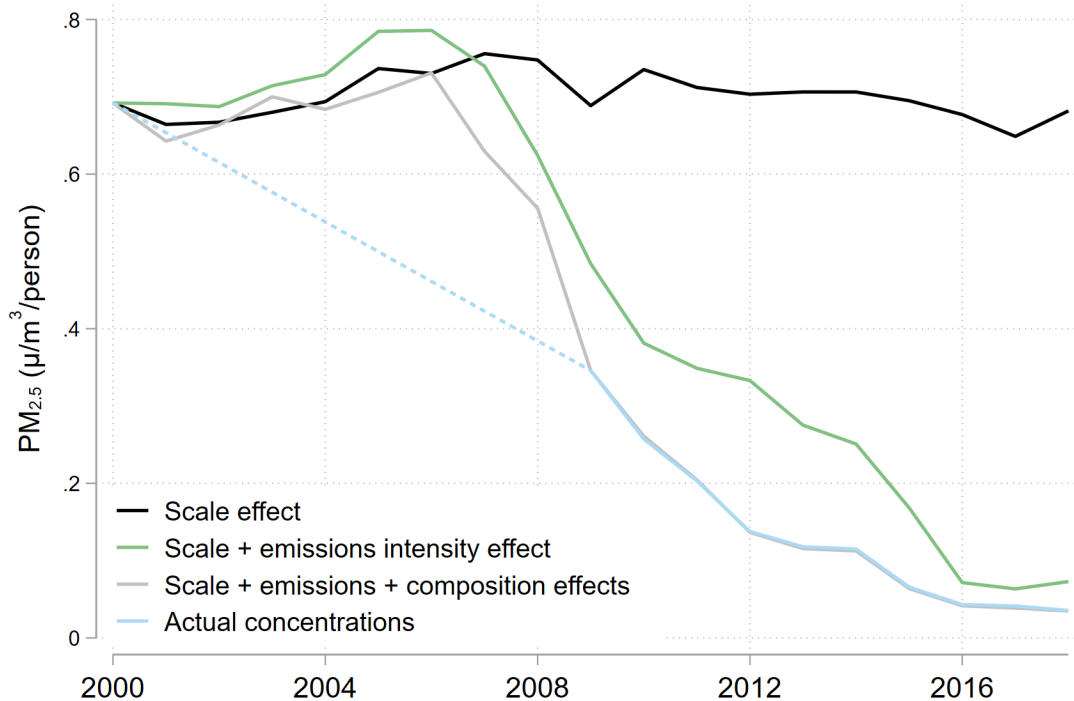
**Figure A5:** Trends in pollution concentrations by income quartiles



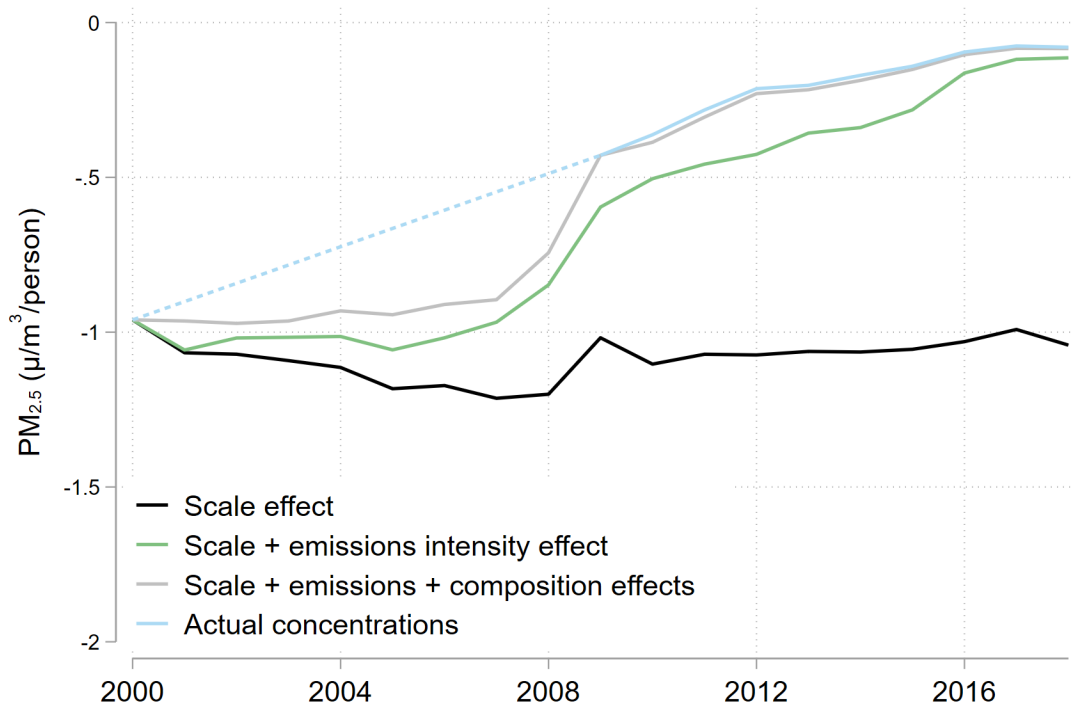
**Notes:** 2000-2018 PM<sub>2.5</sub> concentrations for the average bottom and top quartile individual.

**Figure A6:** Decomposition of pollution disparity trends: coal

(a) Black-White disparity



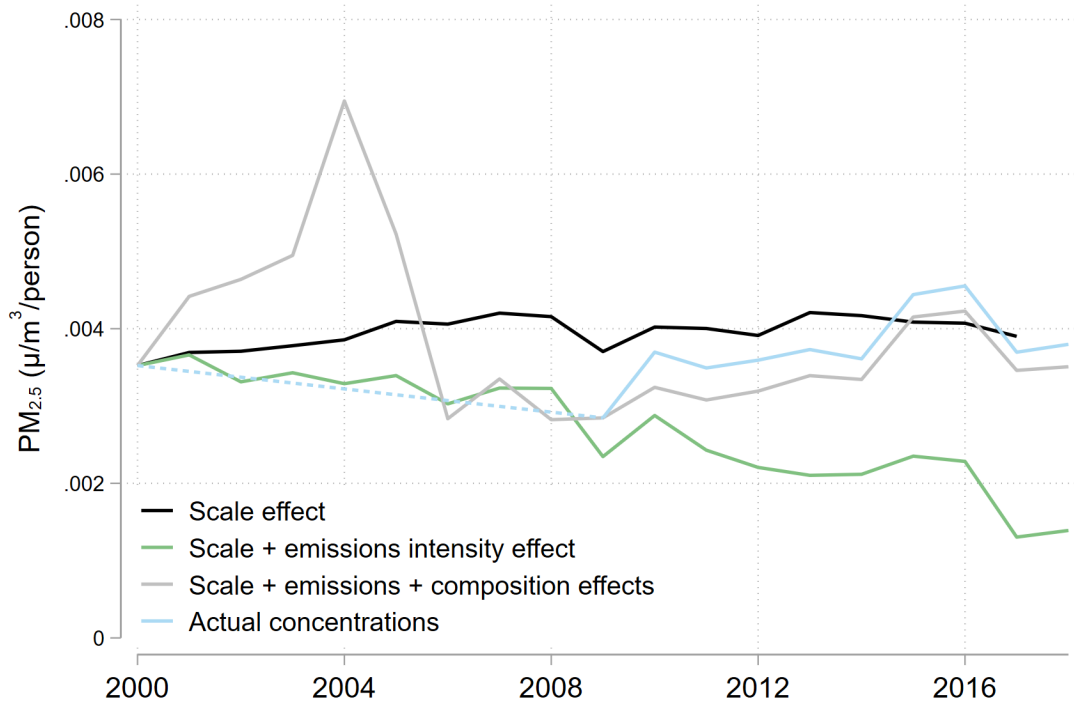
(b) Hispanic-White disparity



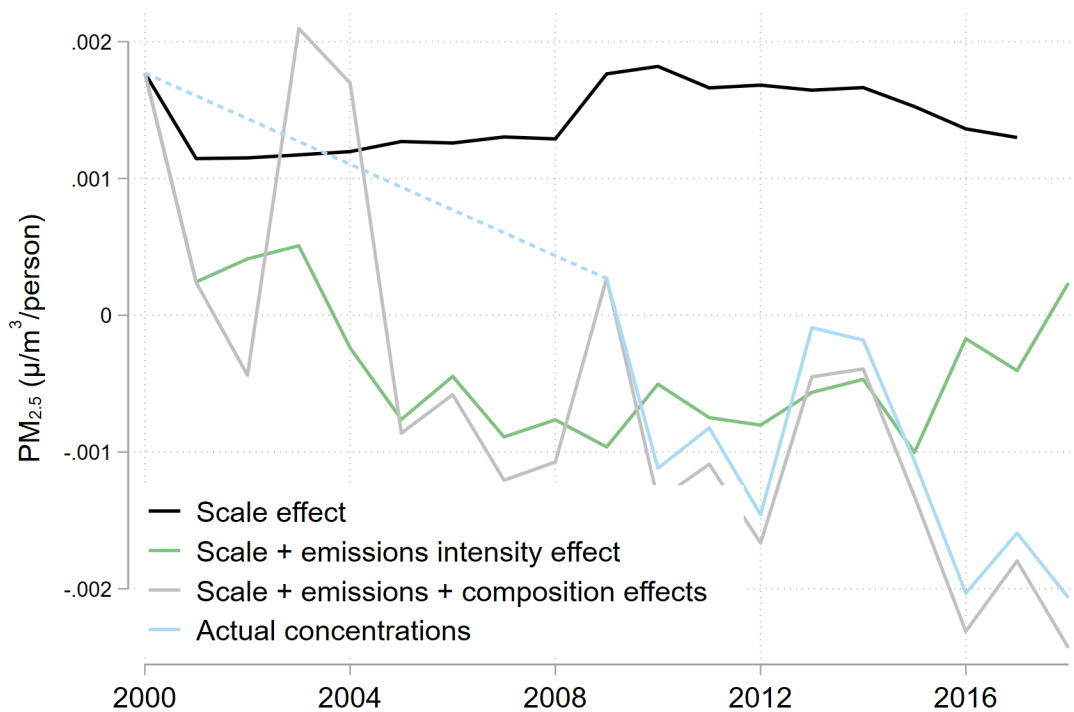
**Notes:** Panel (a) shows the Black-White PM<sub>2.5</sub> disparity trend and its components over 2000-2018 from coal-fired EGUs. Panel (b) shows the Hispanic-White PM<sub>2.5</sub> disparity trend. Dashed line shows interpolated value during 2001-2008 in the absence of census tract-level demographic data.

**Figure A7:** Decomposition of pollution disparity trends: natural gas

(a) Black-White disparity



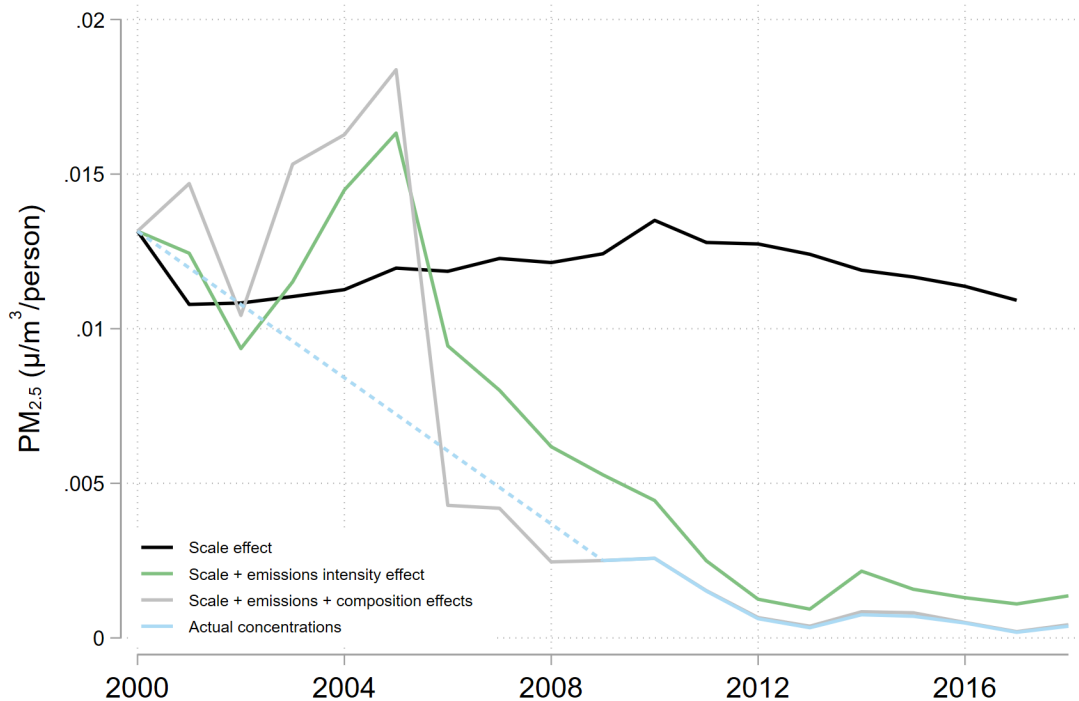
(b) Hispanic-White disparity



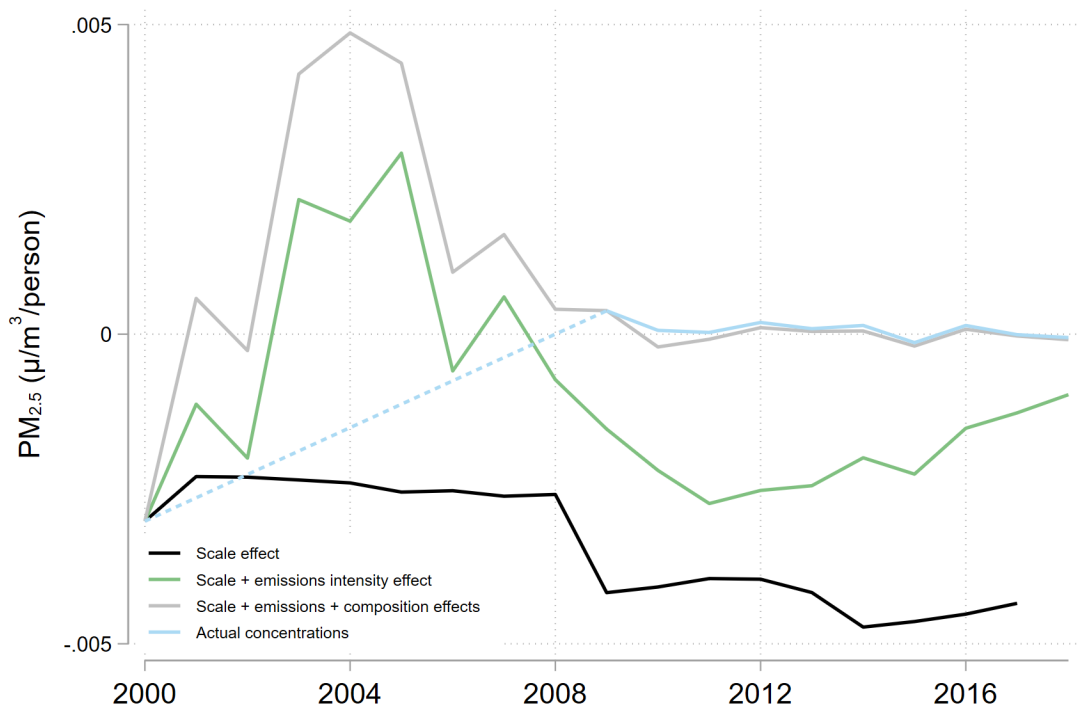
**Notes:** Panel (a) shows the Black-White PM<sub>2.5</sub> disparity trend and its components over 2000-2018 from natural gas-fired EGUs. Panel (b) shows the Hispanic-White PM<sub>2.5</sub> disparity trend. Dashed line shows interpolated value during 2001-2008 in the absence of census tract-level demographic data.

**Figure A8:** Decomposition of pollution disparity trends: oil

(a) Black-White disparity



(b) Hispanic-White disparity



**Notes:** Panel (a) shows the Black-White PM<sub>2.5</sub> disparity trend and its components over 2000-2018 from oil-fired EGUs. Panel (b) shows the Hispanic-White PM<sub>2.5</sub> disparity trend. Dashed line shows interpolated value during 2001-2008 in the absence of census tract-level demographic data.

## Appendix B: Additional Tables

**Table A1:** Electricity Generating Unit and Stack Characteristics

	(1) All	(2) Coal	(3) Natural Gas	(4) Oil
Average Unit Size (MW)	196.49 (200.27)	454.36 (287.39)	159.78 (134.29)	79.36 (145.22)
Heat Input (1,000 MMBtu)	5,437.68 (9629.32)	17,651.12 (16818.49)	3,444.51 (4811.94)	249.29 (935.91)
Annual SO <sub>2</sub> emissions (1,000 kgs)	275.58 (1236.95)	1,597.87 (2613.61)	1.33 (6.84)	9.83 (54.89)
Annual NO <sub>x</sub> emissions (1,000 kgs)	223.49 (637.33)	1,111.68 (1189.19)	49.12 (123.74)	15.14 (41.99)
Temperature at 100% load (K)	403.44 (25.72)	374.52 (38.10)	404.59 (12.10)	443.23 (17.40)
Height (m)	85.74 (46.02)	166.88 (51.84)	64.69 (16.85)	111.39 (12.03)
Velocity at 100% load (m/s)	20.85 (4.38)	23.76 (6.46)	19.82 (3.47)	23.90 (2.15)
Diameter (m)	5.46 (1.46)	7.43 (2.51)	5.04 (0.66)	5.42 (0.45)
Observations	4328	701	3210	417

**Notes:** Column (1) shows the average stack and emissions characteristics for all EGUs. Column (2), (3), and (4) show the average stack and emissions characteristics for coal-, natural gas-, and oil-fired EGUs, respectively.